OPEN

The ISME Journal (2015) 9, 485–496

www.nature.com/ismej

ORIGINAL ARTICLE

Revisiting N_2 fixation in Guerrero Negro intertidal microbial mats with a functional single-cell approach

Dagmar Woebken[1,2,3,8], Luke C Burow[1,2], Faris Behnam[3], Xavier Mayali[4], Arno Schintlmeister[5], Erich D Fleming[2,9], Leslie Prufert-Bebout[2], Steven W Singer[6], Alejandro López Cortés[7], Tori M Hoehler[2], Jennifer Pett-Ridge[4], Alfred M Spormann[1], Michael Wagner[3,5], Peter K Weber[4] and Brad M Bebout[2]

[1]*Departments of Chemical Engineering, and of Civil and Environmental Engineering, Stanford University, Stanford, CA, USA;* [2]*Exobiology Branch, NASA Ames Research Center, Moffett Field, CA, USA;* [3]*Department of Microbiology and Ecosystem Science, Division of Microbial Ecology, University of Vienna, Vienna, Austria;* [4]*Physical and Life Sciences Directorate, Lawrence Livermore National Laboratory, Livermore, CA, USA;* [5]*Large-Instrument Facility for Advanced Isotope Research, University of Vienna, Vienna, Austria;* [6]*Earth Sciences Division, Lawrence Berkeley National Laboratory, Berkeley, CA, USA and* [7]*Laboratory of Geomicrobiology and Biotechnology, Northwestern Center for Biological Research (CIBNOR), La Paz, Mexico*

Photosynthetic microbial mats are complex, stratified ecosystems in which high rates of primary production create a demand for nitrogen, met partially by N_2 fixation. Dinitrogenase reductase (*nifH*) genes and transcripts from *Cyanobacteria* and heterotrophic bacteria (for example, *Deltaproteobacteria*) were detected in these mats, yet their contribution to N_2 fixation is poorly understood. We used a combined approach of manipulation experiments with inhibitors, *nifH* sequencing and single-cell isotope analysis to investigate the active diazotrophic community in intertidal microbial mats at Laguna Ojo de Liebre near Guerrero Negro, Mexico. Acetylene reduction assays with specific metabolic inhibitors suggested that both sulfate reducers and members of the *Cyanobacteria* contributed to N_2 fixation, whereas $^{15}N_2$ tracer experiments at the bulk level only supported a contribution of *Cyanobacteria*. Cyanobacterial and *nifH* Cluster III (including deltaproteobacterial sulfate reducers) sequences dominated the *nifH* gene pool, whereas the *nifH* transcript pool was dominated by sequences related to *Lyngbya* spp. Single-cell isotope analysis of $^{15}N_2$-incubated mat samples via high-resolution secondary ion mass spectrometry (NanoSIMS) revealed that *Cyanobacteria* were enriched in ^{15}N, with the highest enrichment being detected in *Lyngbya* spp. filaments (on average 4.4 at% ^{15}N), whereas the *Deltaproteobacteria* (identified by CARD-FISH) were not significantly enriched. We investigated the potential dilution effect from CARD-FISH on the isotopic composition and concluded that the dilution bias was not substantial enough to influence our conclusions. Our combined data provide evidence that members of the *Cyanobacteria*, especially *Lyngbya* spp., actively contributed to N_2 fixation in the intertidal mats, whereas support for significant N_2 fixation activity of the targeted deltaproteobacterial sulfate reducers could not be found.
The ISME Journal (2015) **9,** 485–496; doi:10.1038/ismej.2014.144; published online 10 October 2014

Introduction

In photosynthetic microbial mats high CO_2 fixation activity often creates a great demand for nitrogen (N), which is partially met by high rates of N_2 fixation (Bebout *et al.*, 1994; Herbert, 1999). It was hypothesized that microbial mat development is dependent on the activity of N_2-fixing microorganisms (diazotrophs) (Bergman *et al.*, 1997). Microbial mats inhabiting the intertidal zone from Laguna Ojo de Liebre (Supplementary Figures S1 and S2) close to Guerrero Negro, Baja California Sur, Mexico, experience frequent alternating periods of desiccation (and thereby aeration) and tidal flooding (Omoregie *et al.*, 2004b; Rothrock and Garcia-Pichel, 2005) and are subject to frequent physical disruption. This environment leads to a 'pioneering stage' of habitat colonization, where N_2 fixation is an important process, providing a source of N for mat growth (Bebout *et al.*, 1994).

Correspondence: D Woebken, Department of Microbiology and Ecosystem Science, Division of Microbial Ecology, University of Vienna, Vienna 1090, Austria.
or BM Bebout, Exobiology Branch, NASA Ames Research Center, Moffett Field, CA 94035, USA.
E-mail: dwoebken@gmail.com or brad.m.bebout@nasa.gov
[8]Current address: Department of Microbiology and Ecosystem Science, Division of Microbial Ecology, University of Vienna, Vienna 1090, Austria.
[9]Current address: California State University Channel Islands, Camarillo, CA 93012, USA.
Received 2 February 2014; revised 15 June 2014; accepted 29 June 2014; published online 10 October 2014

Although N_2 fixation has previously been investigated in the intertidal mats from Laguna Ojo de Liebre (Bebout *et al.*, 1993; Omoregie *et al.*, 2004a, b), the identity of the active diazotrophs remains elusive. Historically, *Cyanobacteria* were believed to be responsible for N_2 fixation in microbial mats given their visual dominance and cultivation without an exogenous N source (Stal and Krumbein, 1981; Stal and Bergman, 1990; Paerl *et al.*, 1991). This was further supported by biogeochemical assays using an inhibitor of oxygenic photosynthesis (3-(3,4-dichlorophenyl)-1,1-dimethylurea (DCMU)) (Stal *et al.*, 1984; Bebout *et al.*, 1993). However, molecular methods indicated that additional microorganisms (such as heterotrophic bacteria) present in microbial mats have the genetic potential for N_2 fixation and may play an important role in microbial mat N_2 fixation (Zehr *et al.*, 1995; Steppe *et al.*, 1996). In particular, sulfate-reducing bacteria (SRB) were hypothesized to contribute to N_2 fixation in microbial mats (Steppe and Paerl, 2002). Indeed, earlier studies of the Laguna Ojo de Liebre intertidal mats, combining biogeochemical and molecular assays, were unable to detect *nifH* genes or transcripts from the visually dominating cyanobacterium *Lyngbya* spp. (Omoregie *et al.*, 2004a, b), despite the fact that several *Lyngbya* spp. possess the capability to fix N_2 in culture (for example, Paerl *et al.*, 1991; Bebout *et al.*, 1993). Instead, *nifH* sequences from Cluster III, including SRB that belong to the *Deltaproteobacteria*, dominated these *nifH* gene libraries and were also found in the transcript library (Omoregie *et al.*, 2004a, b). In addition to these deltaproteobacterial sulfate-reducing diazotrophs, Cluster III also contains sequences from spirochetes, methanogens, acetogens, green sulfur bacteria and *Clostridia* (Zehr *et al.*, 2003). Comparative investigation of available *nifH* sequences indicates that Cluster III contains the greatest diversity of all *nifH* lineages and that its diversity is still not fully understood (Gaby and Buckley, 2011).

The presence and/or transcription of the *nifH* gene does not necessarily mean that an organism actively fixes N_2 in the environment since the nitrogenase enzyme activity can be regulated on multiple levels ranging from transcription (Chen *et al.*, 1998) to post-translational protein modification (Kim *et al.*, 1999). As such, identification of active diazotrophs requires investigation on the functional level, for example through stable isotope probing (SIP) with $^{15}N_2$. The incorporation of ^{15}N into biomass can be directly imaged with secondary ion mass spectrometry (SIMS; Cliff *et al.*, 2002; Lechene *et al.*, 2006; Popa *et al.*, 2007), and especially the NanoSIMS 50 has been used recently to investigate diazotrophic communities at the single-cell level across diverse environments (for example, Dekas *et al.*, 2009; Halm *et al.*, 2009; Foster *et al.*, 2011; Ploug *et al.*, 2011; Woebken *et al.*, 2012).

We sought to identify the diazotrophic community in intertidal mats at Laguna Ojo de Liebre, Mexico, and ascertain using a $^{15}N_2$-SIP single-cell approach the actively N_2-fixing populations. We applied a combination of inhibitor amendment experiments, *nifH* gene and transcript sequencing, and $^{15}N_2$ incubations followed by single-cell isotope measurements. As in previous studies, inhibitor experiments coupled to acetylene reduction assays (ARAs) suggested that *Cyanobacteria* and SRB both have a major role in N_2 fixation. However, further investigations through inhibitor addition experiments combined with $^{15}N_2$-incubations, molecular and NanoSIMS analyses provided strong evidence that members of the *Cyanobacteria* (especially *Lyngyba* spp.) were the most active diazotrophs in the investigated mats.

Materials and methods

Mats with a phototrophic layer dominated by *Lyngbya* spp. (in terms of biomass, as assessed by light microscopy) were sampled from the intertidal zone at Laguna Ojo de Liebre, Baja California, Mexico (27.758 N (Lat.) and −113.986 W (Long.)) on 15 September 2010 (Supplementary Figures S1 and S2) during low tide. The N_2 fixation activity of two replicate mat pieces of ca. 20 cm × 30 cm was investigated over a diel cycle at a nearby field laboratory (outdoor setup in Guerrero Negro, Baja California, performed in acrylic aquaria as described below) from 15 to 16 September 2010. Other mat pieces were transported to the NASA Ames Research Center, CA, USA, on 16 September 2010 for additional diel cycle studies including inhibition experiments, stable isotope incubations as well as nucleic acid-based investigations. For experiments at NASA Ames, mats were placed in acrylic aquaria transparent to ultraviolet radiation and covered with *in situ* water for 2 days before the beginning of the diel study (starting at 1200 hours and ending at 1500 hours the next day). To ensure full photosynthetic activity in the mats during the N_2 fixation experiments, resumption of photosynthetic activity after rewetting was investigated by pulse amplitude modulation fluorescence. The quantum yield of PSII (ΦPSII) for a light-adapted sample was calculated based on F_S (steady-state fluorescence under actinic light) and F_M' (maximum fluorescence under actinic light) measurements using the following equation: $\Phi PSII = (F_M' - F_S)/F_M'$. Rehydrated mats exhibited maximal photosynthetic activity (ΦPSII = 0.30–0.40) within 4 h of wetting in congruence with earlier studies (Fleming *et al.*, 2007); thus, diel cycle studies were conducted with fully active mats. Diel cycle studies were carried out under natural solar irradiance, and the water temperature was kept constant at ∼18 °C.

Nitrogenase activity was measured with ARAs and $^{15}N_2$ incubations as previously described (Bebout *et al.*, 1993; Woebken *et al.*, 2012). For more details see Supplementary Information.

Bulk sample $^{15}N/^{14}N$ isotope ratios were determined by isotope-ratio mass spectrometry (IRMS; ANCA-IRMS, PDZE Europa Limited, Crewe, England) at the University of California, Berkeley, corrected relative to National Institute of Standards and Technology (NIST, Gaithersburg, MD, USA) standards and are expressed as $^{15}N/(^{14}N + ^{15}N)$ isotope fractions, given in at% (means ± s.e.).

All inhibition experiments were conducted at the NASA Ames Research Center. For photosynthesis inhibition experiments, DCMU was added to intact mat slabs before sunrise on the first day of the diel cycle study with a final concentration of 20 μM to ensure complete inhibition of photosystem II (PSII) (Oremland and Capone, 1988). For ARAs or $^{15}N_2$ incubation experiments, mat cores were subsampled from these mat slabs and incubated as described in Supplementary Information, but with *in situ* water containing DCMU. Mat cores from mat slabs without DCMU treatment served as controls and were incubated in seawater without DCMU. For sulfate reduction inhibition experiments, sodium molybdate (Na_2MoO_4, a structural analog of sulfate) was added to intact mat slabs submerged in *in situ* seawater or artificial seawater in the early morning of the first day of the diel cycle study to achieve a final concentration of 30 mM (Oremland and Capone, 1988). Mat slabs incubated in *in situ* seawater or artificial seawater without molybdate served as controls. Two diel experiments were conducted: (A) mat samples in *in situ* seawater (control) versus mat samples in molybdate-amended seawater; and (B) mat samples in artificial seawater containing 23 mM sulfate (control) versus mat samples in artificial seawater without sulfate and with added molybdate. Incubations for ARA or $^{15}N_2$ experiments were conducted as described in Supplementary Information.

All diel cycle experiments were accompanied by mat sampling for molecular analysis. At multiple time points during a diel experiment, four mat cores of 1 cm diameter were flash frozen in liquid nitrogen and stored at −80 °C until further processing. DNA and RNA extractions were conducted as previously described (Woebken *et al.*, 2012) and are further described in Supplementary Information. As N_2 fixation was observed only during the night, all sequence data were derived from night-time samples.

454 pyrotag amplicon libraries (V6–V8 region) and clone libraries for Sanger sequencing of 16S rRNA genes/transcripts from two biological replicate mats, as well as clone libraries of the *nifH* genes/transcripts, were constructed and analyzed as previsously described (Woebken *et al.*, 2012). Detailed information about the construction and analysis of these libraries can also be found in Supplementary Information. 16S rRNA 454 pyrotag sequencing resulted in 20 616 and 15 524 reads from both DNA templates and 20 138 and 22 246 reads from both cDNA templates (Supplementary Table S1). 16S rRNA Sanger sequencing resulted in 520 sequences from DNA samples (D3 = 256 and D5 = 264 sequences) and 316 sequences from cDNA samples (C3 = 150 and C5 = 166 sequences). Regarding *nifH* sequences, 313 sequences were retrieved from DNA, 522 sequences from cDNA and 181 from cDNA of the molybdate inhibition experiment. 16S rRNA and 16S rRNA gene sequences obtained in this study are deposited in GenBank under accession numbers KJ997979–KJ998814. Sequences of *nifH* genes and transcripts are deposited in GenBank under accession numbers KM212180–KM212266.

Single-cell NanoSIMS analyses were performed to identify active diazotrophs. The upper 2 mm of paraformaldehyde-fixed mat samples from $^{15}N_2$ incubation experiments and negative control mat cores were prepared on 5 mm × 5 mm silicon wafer pieces (Ted Pella, Redding, CA, USA) for NanoSIMS analysis as previously described (Woebken *et al.*, 2012). Filamentous cyanobacteria (*Lyngbya* spp.-related and small filamentous cyanobacteria) were identified based on their red autofluorescence when illuminated with green light by epifluorescence microscopy (excitation: BP 546/12, beam splitter: FT 560, emission: BP 607/80) and based on their morphology, as imaged by scanning electron microscopy (SEM; FEI Inspect F, FEI, Hillsboro, OR, USA). *Deltaproteobacteria* were stained by catalyzed reporter deposition-fluorescence *in situ* hybridization (CARD-FISH) as previously described (Pernthaler *et al.*, 2002; Woebken *et al.*, 2012) using probes DELTA495 a-c (Loy *et al.*, 2002; Lücker *et al.*, 2007). Stained cells were identified and localized by epifluorescence microscopy. All targeted cells were localized and imaged by reflected light microscopy and SEM to ensure that the target cells were free of overlying cells or other material so that $^{15}N/^{14}N$ ratios could unambiguously be attributed to the target cells. SIMS analysis was performed at the Lawrence Livermore National Laboratory (LLNL) using a NanoSIMS 50 (Cameca, Gennevilliers Cedex, France) as previously described (Woebken *et al.*, 2012). Isotopic compositions are expressed as the abundance of the tracer relative to the total tracer element ($a_N = ^{15}N/(^{14}N + ^{15}N)$) in at%. Reported data refer to the arithmetic mean of all measurements per cell type ± s.e. Detailed methods are provided in Supplementary Information.

Data retrieved in the ARAs, IRMS data of vertical sections and inhibition experiments as well as NanoSIMS data were analyzed for significant differences using Student's *t*-test or analysis of variance (ANOVA) with an alpha error of 0.05 and the Tukey–Kramer honestly significant difference as a multiple means comparison test (JMP Version 7, SAS Institute Inc., Cary, NC, USA). Normal distribution was tested with the Shapiro–Wilk *W*-test, and in cases where the data did not meet the standard of homogeneity of variance, the Welch ANOVA was used to confirm the initial result. As ^{15}N enrichment

levels were very low in *Deltaproteobacteria* measured by NanoSIMS, the natural abundance values for *Deltaproteobacteria* were used to test for significant enrichment based on a 95% confidence interval.

Results

Bulk-level N_2 fixation analysis

Nitrogenase activities in ARAs were significantly higher during the night than during the day-time (average ± s.d. 131 ± 67 vs 5 ± 7 μmol C_2H_4 m^{-2} h^{-1}, $P<0.0001$, Figure 1a) and well within the range of previously reported rates (Bebout *et al.*, 1994; Omoregie *et al.*, 2004b). The potential contribution of oxygenic phototrophs to N_2 fixation was investigated by inhibiting photosystem II (PSII) with DCMU. In experiments where DCMU was added before sunrise on the first day of a diel experiment, nitrogenase activities were significantly reduced compared to un-amended control incubations (average ± s.d.: 11 ± 3 vs 66 ± 22 C_2H_4 m^{-2} h^{-1}, $P<0.0001$, Figure 1b). The potential contribution of SRB to N_2 fixation was investigated by adding the sulfate reduction inhibitor molybdate. Samples exposed to molybdate had lower nitrogenase activities compared to un-amended incubations (average ± s.d.: 12 ± 5 vs 63 ± 35 C_2H_4 m^{-2} h^{-1}, $P<0.0001$, Figure 1c).

N_2 fixation activity (that is, net ^{15}N incorporation) in the intertidal mats was directly assessed with $^{15}N_2$ incubation experiments (for 10 h in the dark) and subsequent IRMS analysis of both upper and lower mat layers (0 to 2 mm and 2 to 4 mm, respectively). The upper layer was significantly enriched in ^{15}N relative to the deeper layer (Figure 2; average ± s.e.: 0.486 ± 0.023 vs 0.373 ± 0.001 at% ^{15}N, $P<0.001$). Mat cores incubated in air without $^{15}N_2$ served as control samples for natural abundance and had values of (average ± s.e.) 0.371 ± 0.001 (0 to 2 mm) and 0.373 ± 0.001 (2 to 4 mm) at% ^{15}N. On the basis of these results, we focused all additional analyses on the upper layer. In $^{15}N_2$ incubation experiments of this upper layer with and without inhibitors, mats incubated with DCMU had significantly lower ^{15}N incorporation relative to control incubations without DCMU (Figure 2; average ± s.e.: 0.380 ± 0.007 vs 0.452 ± 0.021 at% ^{15}N, $P<0.05$). In molybdate addition experiments, incubations where molybdate was added had a slightly lower ^{15}N enrichment than un-amended mats (average ± s.e.: 0.429 ± 0.013 vs 0.466 ± 0.015 at% ^{15}N, $P=0.063$), but the difference was not significant at the $P<0.05$ level.

Microbial diversity based on 16S rRNA and 16S rRNA gene analysis

Lyngbya spp. and other filamentous cyanobacteria dominated the biomass of the upper phototrophic layer of the microbial mats from Laguna Ojo de Liebre based on light micrographs (Supplementary

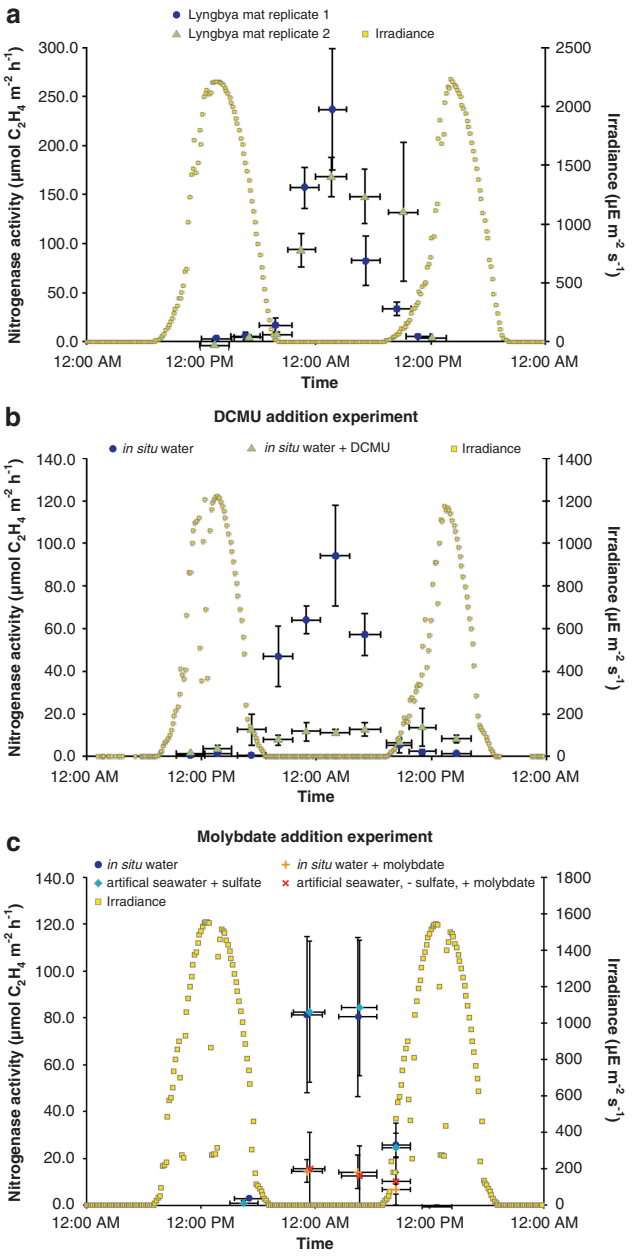

Figure 1 Acetylene reduction assay (ARA) as a proxy for N_2 fixation activity in intertidal microbial mats from Laguna Ojo de Liebre, Baja California, Mexico. Each time point measurement in each diel cycle experiment was conducted in triplicate (values in graphs depict the average of the three replicate measurements per time point per experiment including the s.d. as error bars). The horizontal bars indicate the incubation intervals of mat cores with acetylene in the ARA (incubation time was 3 h). (**a**) The diel cycle experiment was conducted in Guerrero Negro, Mexico, before the mats were transported to CA, USA, for detailed analysis. Two replicate diel cycle experiments are shown in the graph. (**b**, **c**) Diel cycle experiments of intertidal mats from Laguna Ojo de Liebre conducted in the laboratory at NASA Ames, CA, USA. Note the reduced N_2 fixation rates of controls ('*in situ* water') compared to the experiments in Guerrero Negro. (**b**) Experiment investigating the effect of DCMU on nitrogenase activity. (**c**) Experiment investigating the effect of molybdate on nitrogenase activity. No significant difference was detected in control ARAs conducted with *in situ* water versus artificial seawater (average ± s.d.: 63 ± 36 vs 64 ± 36 C_2H_4 m^{-2} h^{-1}, $P=0.3386$).

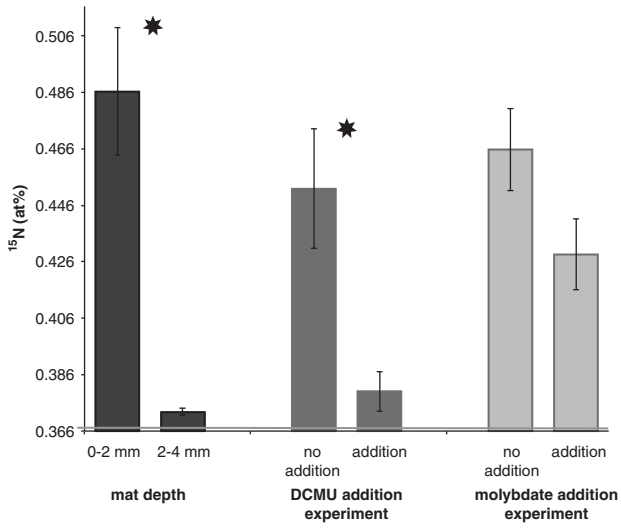

Figure 2 ^{15}N enrichment (at%) of mat cores that were incubated with $^{15}N_2$ for 10 h in the dark measured by IRMS. Average values of three biological replicates per treatment are depicted with standard errors (for '0 to 2 mm depth', $n=10$). Asterisks indicate significant different paired treatments at $P<0.05$. Natural abundance of 0.37 at% ^{15}N is indicated by a gray horizontal line.

Figure S3). However, 16S rRNA and 16S rRNA gene sequencing indicated that the microbial community of this layer was diverse and composed of multiple bacterial phyla (Figure 3 and Supplementary Table S2). DNA-derived Sanger sequences were affiliated with nine different phyla based on the RDP classifier (Wang *et al.*, 2007). The majority of DNA sequences were classified as *Proteobacteria* (30–36%) and *Bacteroidetes* (17–33%), followed by *Chloroflexi* (6–12%), *Cyanobacteria* (5–9.5%) and *Verrucomicrobia* (1–9.5%). In contrast, the majority of 16S rRNA sequences (cDNA-based) grouped with *Cyanobacteria* (57–62%), followed by *Proteobacteria*, *Chloroflexi* and *Bacteroidetes* (6–20%). Based on phylogenetic analyses, all 16S rRNA cyanobacterial sequences were related to filamentous cyanobacteria (Supplementary Figure S4), and 24.4% of these cyanobacterial 16S rRNA sequences were related to *Lyngbya* spp., with up to 98.7% sequence identity to *Lyngbya aestuarii* PCC 7419 and *Lyngbya* sp. PCC 8106, or 97.9% identity to *Lyngbya majuscula* CCAP. 454 pyrotag amplicon sequencing was used to investigate the 16S rRNA and 16S rRNA gene diversity with greater coverage, and revealed reads clustering in 15 phyla (Figure 3 and Supplementary Table S2). However, the trend was the same as in Sanger-based sequences (Figure 3); most of the amplicons recovered from DNA were assigned to *Proteobacteria*, *Chloroflexi*, *Cyanobacteria* and *Bacteroidetes*, while the majority of reads originating from cDNA clustered with *Cyanobacteria*. Calculation of the Chao1 estimator and the Shannon index revealed greater diversity in DNA-based reads than in cDNA-based reads (Supplementary Table S1).

Community analysis of potential diazotrophs (nifH gene and transcript analysis)

The diversity of bacteria with the genetic capability to fix N_2 was specifically analyzed by sequencing *nifH* genes and transcripts from the upper 2 mm of the intertidal mats. Deduced amino-acid sequences formed 87 OTUs based on a cutoff of 97% sequence identity. Phylogenetic analysis of the deduced (amino-acid) NifH sequences derived from extracted DNA revealed that the majority (64.2%) grouped with Cluster III (based on Zehr *et al.*, 2003; with uncultured microorganisms and *Deltaproteobacteria*), and the rest with Cluster I (with *Cyanobacteria*, *Alpha-*, *Gamma-* and *Betaproteobacteria*) (Figure 4). To focus on the community that was expressing the *nifH* gene, we also analyzed sequences derived from extracted RNA after reverse transcription into cDNA. The majority of these sequences (80.8%) were related to *Cyanobacteria* forming three major groups (*Lyngbya* spp.-cluster, cyanobacterial cluster 1 and 2, Figure 4 and Supplementary Figure S5), with *Lyngbya* spp.-related sequences being the most abundant. The other two abundant groups of cyanobacterial sequences clustered with sequences of filamentous cyanobacteria such as *Phormidium* and *Leptolyngbya*, and sequences from other microbial mats, freshwater, sponge or sediment samples. A minor proportion of the cyanobacterial *nifH* sequences (0.2%) were related to a cyanobacterium that is a dominant diazotroph in mats of Northern California (ESFC-1; Woebken *et al.*, 2012; Everroad *et al.*, 2013). Of all cDNA-based sequences, 16.9% grouped with Cluster III (1.3% of all sequences with deltaproteobacterial clusters containing known SRB and 15.5% with unclassified Cluster III sequences).

NifH clone libraries (based on cDNA) of samples from the molybdate addition experiments were almost completely comprised of cyanobacterial sequences (97.2%), and only a minor portion of the sequences clustered with Cluster III (1.7%) or *Deltaproteobacteria* within this cluster (0.6%). Mat samples treated with DCMU during the diel cycle study failed to produce any detectable PCR product from cDNA with *nifH*-targeting primers (tested in two replicate RNA extractions, see Supplementary Information for details).

Single-cell isotope analysis of potential diazotrophic microbial community members

Based on the results of the inhibitor addition experiments and sequencing of expressed *nifH* genes, we focused our single-cell isotope analyses on *Cyanobacteria* and *Deltaproteobacteria*. The latter group was targeted to test as broadly inclusive as possible the $^{15}N_2$ fixation activity of SRB within the *Deltaproteobacteria*. All detected *Cyanobacteria* were filamentous, and *Lyngbya* spp. filaments were easily distinguishable from other filamentous cyanobacteria based on their morphology (Supplementary Figure S3). The highest ^{15}N

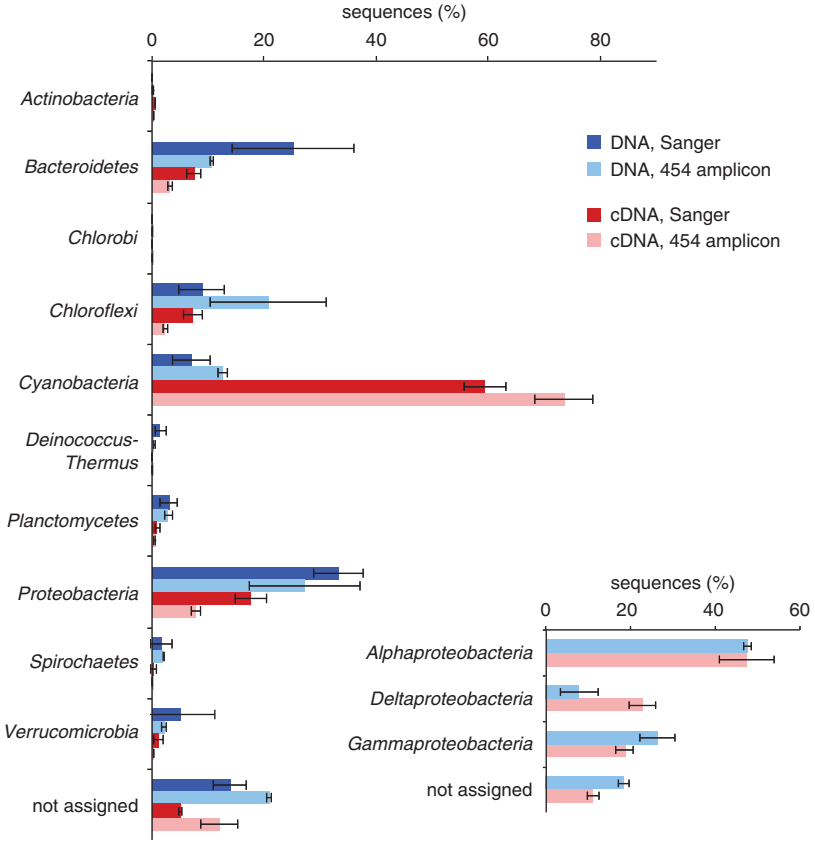

Figure 3 Microbial community analysis based on 16S rRNA gene and transcript sequencing of the upper 2 mm of intertidal mats at Laguna Ojo de Liebre. Phyla depicted are those that contain ⩾0.1% of sequences detected by either Sanger sequencing (dark blue and dark red bars) or 454 amplicon sequencing (bars in light blue and light red). Each bar depicts the average value of 2 biological replicates. Both approaches illustrate a diverse community based on DNA analysis, with most of the sequences grouping within *Proteobacteria*, *Bacteroidetes*, *Chloroflexi* and *Cyanobacteria*. Sequences based on cDNA are strongly dominated by *Cyanobacteria* (up to 74% of the sequences), followed by *Proteobacteria*, *Bacteroidetes* and *Chloroflexi*. Inlet depicts proteobacterial community composition based on 454 amplicon sequences (sequence abundance of *Alpha-*, *Delta-* and *Gammaproteobacteria* within the *Proteobacteria*).

enrichments in these mats were measured in *Lyngbya* spp. filaments (maximum of 14.54 at%), with an average (±s.e.) ^{15}N tracer content of 4.40 ± 0.57 at% (Figure 5, Supplementary Table S3). The enrichment in *Lyngbya* spp. filaments was significantly higher than in any other analyzed cells ($P<0.0001$ compared to small filamentous cyanobacteria; $P<0.0001$ compared to *Deltaproteobacteria*; and $P=0.01$ compared to unidentified single cells). Smaller filamentous cyanobacteria had an average enrichment (±s.e.) of 0.60 ± 0.02 at% ^{15}N with a maximum of 1.32 at%. The ^{15}N enrichment of CARD-FISH-stained deltaproteobacterial cells from $^{15}N_2$-labeled mats was not significantly different from those in control mat samples (average ± s.e.: 0.38 ± 0.00 vs 0.37 ± 0.00 at% ^{15}N, $P=0.170$). The highest ^{15}N enrichment measured in an individual deltaproteobacterial cell was 0.41 at%.

Discussion

Members of the *Proteobacteria*, *Bacteroidetes*, *Chloroflexi* and *Cyanobacteria* dominated the investigated mats based on 16S rRNA gene sequences (Figure 3), yet members of the *Cyanobacteria* mostly comprised the active microbial community (as inferred by 16S rRNA sequence-based community analysis). This dominance of cyanobacterial sequences in libraries derived from RNA seems to be common for microbial mats containing large filamentous cyanobacteria and was previously described (Burow *et al.*, 2012, 2013; Lee *et al.*, 2014). A similar pattern was observed for the *nifH* sequence analysis; sequences of Cluster III (including known SRB) dominated the DNA sequence pool, whereas cyanobacterial sequences dominated by far the pool of expressed *nifH* genes while the proportion of Cluster III sequences was strongly decreased. These data are in disagreement with earlier studies of mats from Laguna Ojo de Liebre in which *nifH* gene and transcript analyses suggested that both *Cyanobacteria* and *Deltaproteobacteria* (including SRB) were the major contributors for N_2 fixation (Omoregie *et al.*, 2004a, b; Moisander *et al.*, 2006). Interestingly, our detected *nifH* sequences in Cluster I and Cluster III, specifically sequences related to *Lyngbya* spp.

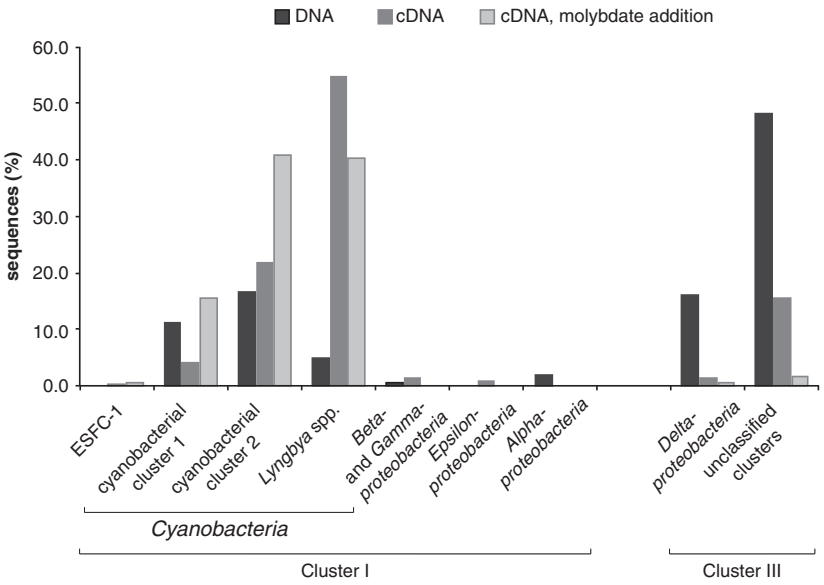

Figure 4 Taxonomic classification of deduced (amino-acid) NifH sequences derived from DNA (*nifH* genes) and RNA (cDNA, *nifH* transcripts) in the upper 2 mm layer of intertidal microbial mats from Laguna Ojo de Liebre. Sequences derived from DNA are depicted in black ($n = 313$), from cDNA in dark grey ($n = 522$) and from cDNA of molybdate-treated samples in light grey ($n = 181$). PCR amplification of cDNA from the DCMU treatment yielded no products.

were not detected in these previous studies. This lack of congruence could reflect temporal differences in the microbial community at the time studied (2001–2010), as these mats are characterized by a 'pioneering life style' (Bebout *et al*., 1993) and thereby will most likely be dynamic in their microbial community composition. Other explanations for the differences in the detected microbial communities could be the depth of sequencing or a bias in the nucleic acid extraction. Although the same primer set was used in all studies (Zehr and Turner, 2001), in our study we added a pre-homogenization step prior to nucleic acid extraction, which could have increased the lysis efficiency of *Lyngbya* spp. cells.

The application of inhibitors in diel cycle studies can suggest the contribution of certain functional groups to N_2 fixation, an approach that has been used extensively in the past (for example, Stal *et al.*, 1984; Griffiths and Gallon, 1987; Bebout *et al*., 1993; Pinckney and Paerl, 1997; Steppe and Paerl, 2002). The addition of DCMU, an inhibitor of oxygenic photosynthesis (Oremland and Capone, 1988), during the day-time photoperiod strongly and significantly decreased N_2 fixation the subsequent night, based on ARAs (Figure 1b) and $^{15}N_2$ incubation experiments (Figure 2). This pattern was previously observed in non-heterocystous cyanobacterial mats (Griffiths and Gallon, 1987; Bebout *et al*., 1993), and also in *Lyngbya* spp. cultures (Bebout *et al*., 1993). DCMU interrupts the photosynthetic electron flow by inhibiting the O_2-evolving PS II, which depletes the reductant formation required for N_2 fixation (Oremland and Capone, 1988). This decrease in reductant will most likely also prevent CO_2 fixation (Bebout *et al*., 1993; Paerl *et al*., 1996; Pinckney and Paerl, 1997), leading to a shortage of organic storage compounds that can be used for N_2 fixation. This combined shortage in reductant can explain the observed decrease in N_2 fixation rates upon DCMU addition and suggests that members of the *Cyanobacteria* contributed to N_2 fixation activity.

This observation was supported by the detection of expressed cyanobacterial *nifH* genes in untreated control mats that showed N_2 fixation (Figure 4). *NifH* transcripts related to *Lyngbya* spp. dominated the transcript pool, indicating that in these mats *Lyngbya* spp. were actively expressing *nifH* and potentially fixing N_2. In addition, in DCMU-treated mats, we were unable to PCR amplify *nifH* transcripts, which is in congruence with a strong inhibition of N_2 fixation activity in the DCMU addition experiment as observed in ARAs and $^{15}N_2$ incubations followed by IRMS. Together, inhibitor experiments and sequence data suggested that *Cyanobacteria* were actively fixing N_2 in the investigated mats, especially members of *Lyngbya* spp. However, care must be taken to infer N_2 fixation activity from detected *nifH* transcripts or relative sequence abundance. First, nitrogenase enzyme activity can be regulated after transcription until the post-translational level (Kim *et al*., 1999). Furthermore, the potential for PCR biases (Suzuki and Giovannoni, 1996; Polz and Cavanaugh, 1998) makes it difficult to infer the activity of certain groups based on their *nifH* transcript abundance. Therefore, direct N_2 fixation measurements coupled to the identification of cells are needed to clearly identify active diazotrophs in environmental samples. Incubation experiments with $^{15}N_2$ and

single-cell isotope analysis through NanoSIMS allowed us to investigate the active diazotrophs by measuring the incorporation of ^{15}N into cellular biomass. This analysis revealed ^{15}N enrichment in filamentous cyanobacteria of different morphotypes (Figures 5a–c), which corresponded to multiple detected clusters of cyanobacterial *nifH* sequences (Supplementary Figure S5). Consistent with the result of the *nifH* transcript analysis, within the filamentous cyanobacteria, *Lyngbya* spp. had by far the highest enrichments in ^{15}N, demonstrating that *Lyngbya* spp. were the most active cyanobacterial diazotrophs in this mat. As previously detected in other diazotrophic populations (Lechene *et al.*, 2007; Woebken *et al.*, 2012), we observed large variations in ^{15}N enrichments of *Lyngbya* spp.

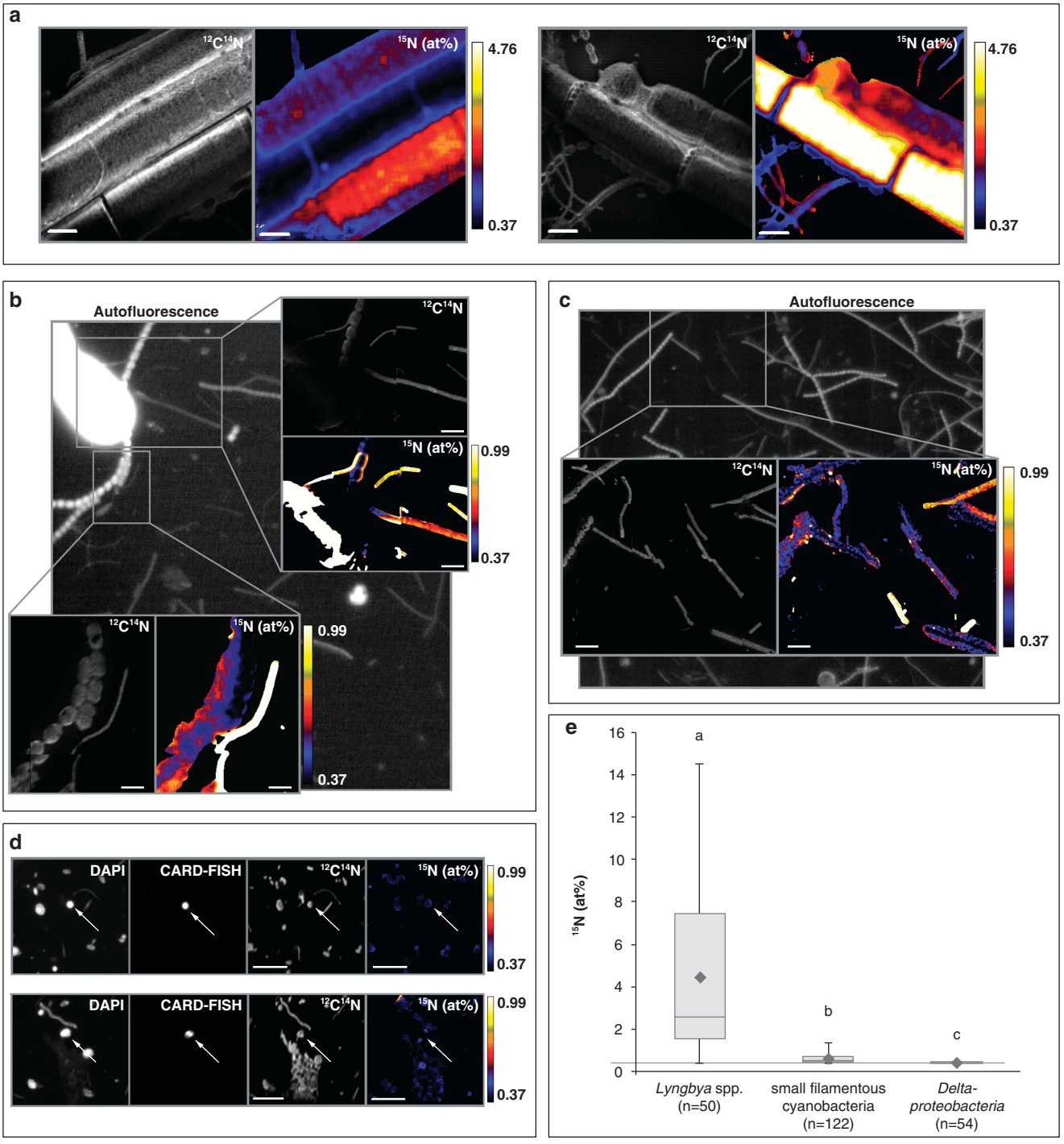

filaments indicating differing N_2 fixation activities. A possible explanation could be spatial heterogeneity in the local environment.

In this study, we sought to take a function-based approach to investigate previous reports that SRB were contributing to N_2 fixation in this mat type (Omoregie *et al.*, 2004a, b; Moisander *et al.*, 2006). In a parallel study, our group measured significant sulfate reduction (as sulfide production) in these same mat samples (Lee *et al.*, 2014). Therefore we can conclude that the sampled mats contained SRB that were physiologically active and that sulfate reduction was not inhibited on account of sampling and transport to the laboratory. On the intertidal flats at Laguna Ojo de Liebre, the mats experience naturally frequent alternating periods of desiccation (leading to aeration) and tidal flooding (Javor and Castenholz, 1984; Omoregie *et al.*, 2004b; Rothrock and Garcia-Pichel, 2005). It appears that SRB in these mats are tolerant against oxygen exposure and maintain their capacity for sulfate reduction even after long oxic periods. The oxygen tolerance of SRB is a phenomenon previously described in cultured SRB and different mats (Canfield and Des Marais, 1991; Minz *et al.*, 1999; Baumgartner *et al.*, 2006; Fike *et al.*, 2008). Detection of expressed *dsrA* genes (a key functional gene for sulfate reduction) by Lee *et al.* (2014) in the mats supports our conclusion that SRB were active, and sequencing revealed that the vast majority of the SRB that expressed *dsrA* (97%) belonged to previously known clusters within the *Deltaproteobacteria* (to *Desulfobacteraceae* and *Desulfovibrionales*). Sequences assigned to the *Desulfobacterales* (*Desulfobacteraceae*) and *Desulfovibrionales* (*Desulfohalobiaceae*) were also identified through 16S rRNA sequencing. These data further support our focus on deltaproteobacterial SRB in our single-cell isotope measurements. We are aware of the possibility that non-deltaproteobacterial heterotrophic diazotrophs exist in these mats, for example related to unidentified groups in Cluster III (designated 'unclassified clusters'; Figure 4). Unfortunately, owing to lack of isolates in these clusters, these bacteria are unidentified at the 16S rRNA level and thus cannot be targeted by a FISH-NanoSIMS approach.

Adding molybdate to the mats resulted in reduced nitrogenase activities in ARAs compared to un-amended samples (Figure 1c). Molybdate serves as a structural analog of sulfate and blocks the sulfate activation, thereby depleting ATP pools in SRB and ultimately causing death (Oremland and Capone, 1988). This effect of molybdate in ARAs was previously observed in an intertidal photosynthetic mat, where molybdate inhibited night-time nitrogenase activity by as much as 64% (Steppe and Paerl, 2002). However, it was previously recognized that reduced N_2 fixation rates in response to molybdate additions could result from many direct effects, but also indirect consequences, such as altered environmental conditions due to the inhibition of sulfide production (Steppe and Paerl, 2002). Results based on this 'specific inhibitor' should be interpreted with caution, a conclusion further supported by our study. In mats from Laguna Ojo de Liebre, the effect of molybdate on overall N_2 fixation rates was only significant in ARAs, whereas $^{15}N_2$ incubation experiments revealed a much less pronounced (and not significant) effect (Figure 2). This observed difference in the effect based on the applied assays could conceivably be caused by an enhanced consumption of ethylene, the measured product in ARAs, in molybdate-treated mats relative to un-amended controls. Ethylene can be metabolized aerobically (de Bont, 1976), and anaerobically (Koene-Cottaar and Schraa, 1998) by microorganisms, and especially the possibility of methanogens reducing ethylene (Oremland, 1981; Elsgaard, 2013) should be mentioned in experiments where SRB are inhibited. Thus, enhanced ethylene consumption in the molybdate treatments could mistakenly be interpreted as a large contribution of SRB to N_2 fixation.

Figure 5 Single-cell isotope measurements by NanoSIMS of $^{15}N_2$-incubated mat samples from Laguna Ojo de Liebre. (**a**) Elemental composition images ($^{12}C^{14}N$ and ^{15}N at%) of *Lyngbya* spp. filaments. However, as described in Supplementary Information, image analysis of *Lyngbya* spp. was not suitable for quantitative analysis of these large cells (instead isotope enrichment measurements were done by accelerated sputtering utilizing high primary ion beam currents (~1 nA, 2 μm beam size)). Therefore, ^{15}N isotopic composition depicted in these images will be an underestimation of the actual enrichment in ^{15}N. (**b**, **c**) Epifluorescence micrograph and elemental composition images ($^{12}C^{14}N$ and ^{15}N at%) of analyzed small filamentous cyanobacteria. Filamentous cyanobacteria were identified based on their autofluorescence. (**d**) NanoSIMS analysis of *Deltaproteobacteria*. Epifluorescence micrographs depict cells stained by DAPI and deltaproteobacterial cells stained by CARD-FISH (with probe-mix DELTA495 a–c). Also depicted are elemental composition images ($^{12}C^{14}N$ and ^{15}N at%). (**e**) Boxplot diagram summarizing all measurements of the three cell types. The number of cells (or individual filaments) analyzed per cell type are indicated. ^{15}N enrichments are depicted in at%; natural abundance is 0.37 at% (indicated by a horizontal line). Lowercase letters indicate significantly different isotopic compositions between different cell types. *Deltaproteobacteria* were not significantly enriched in ^{15}N relative to controls (average of 0.38 vs 0.37 at% ^{15}N, $P=0.170$). The highest ^{15}N enrichment measured in an individual deltaproteobacterial cell was 0.41 at%. Also when ^{15}N dilution through CARD-FISH is accounted for, the deltaproteobacterial ^{15}N isotope fraction values increase only slightly, and their corrected values are still not significantly enriched above natural abundance values (average of 0.38 at% ^{15}N, $P=0.131$). We also considered the individual measured values (as opposed to the population mean), and found that based on the uncorrected values, 20.4% of the cells are significantly enriched in ^{15}N based on a 95% confidence interval. This number increases to 31.5% if the dilution through CARD-FISH is taken into account. Scale bars represent 5 μm. Please note the different scales for ^{15}N at% values.

In this study, molybdate addition experiments coupled with $^{15}N_2$ incubations and IRMS analyses did not indicate a significant contribution of SRB to N_2 fixation, whereas earlier studies suggested that *Deltaproteobacteria* in *nifH* Cluster III, and more specifically SRB within the *Deltaproteobacteria*, were potentially important diazotrophs in photosynthetic mats (Steppe and Paerl, 2002; Omoregie *et al.*, 2004a, b). Sequencing of *nifH* genes and transcripts in our study indicated that sequences of Cluster III (including known SRB) dominated the DNA sequence pool, whereas cyanobacterial sequences dominated vastly the pool of expressed *nifH* genes, and the proportion of Cluster III sequences was strongly decreased (Figure 4). On account of potential PCR biases, one can only interpret the data semiquantitatively; however, these observations suggest that members of the *Cyanobacteria* were more actively expressing *nifH* genes than SRB within Cluster III. This hypothesis is supported by our NanoSIMS analyses, in which *Deltaproteobacteria* were not significantly enriched in ^{15}N relative to controls (average of 0.38 vs 0.37 at% ^{15}N, $P=0.170$). These cells were stained by CARD-FISH in contrast to the *Cyanobacteria*, which could introduce ^{14}N-containing compounds during the procedure leading to a dilution of ^{15}N and thereby to an underestimation of the ^{15}N enrichment. Therefore, we analyzed the effect of CARD-FISH on the ^{15}N (and for completeness also ^{13}C) isotope content in isotopically labeled reference cells (*Escherichia coli* and *Bacillus subtilis*) and detected significantly reduced ^{15}N and ^{13}C isotope contents in these cells by NanoSIMS measurements ($P<0.001$, Supplementary Figures S6–S8, Supplementary Tables S4–S6; experiments are explained in detail in Supplementary Information). Our data indicate that CARD-FISH can result in an apparent dilution of up to 28% for N (and 38% for C). By using these data (28% dilution as a worst-case scenario for N), we tested whether the ^{15}N isotope enrichments measured in microbial mat *Deltaproteobacteria* were strongly influenced by CARD-FISH (see Supplementary Information for calculations and discussion). On the basis of these calculations, when the CARD-FISH ^{15}N dilution is accounted for, the deltaproteobacterial ^{15}N isotope fraction values increase only slightly, and their corrected values are still not significantly enriched above natural abundance values (average of 0.38 at% ^{15}N, $P=0.131$). We also considered the individual measured values (as opposed to the population mean), and found that, based on the uncorrected values, 20.4% of the cells are significantly enriched in ^{15}N based on a 95% confidence interval. This number increases to 31.5% if the dilution through CARD-FISH is taken into account. However, the levels of enrichments were very low compared to the values measured in *Cyanobacteria*. We conclude that even though CARD-FISH has an effect on the ^{15}N isotopic composition, the ^{15}N enrichment values of investigated *Deltaproteobacteria* in this study changed very little when CARD-FISH dilution was accounted for.

Based on this combined approach of inhibitor addition experiments, *nifH* gene and transcript sequencing, and $^{15}N_2$ incubations coupled with single-cell isotope analysis, we did not find support that the analyzed deltaproteobacterial SRB contributed significantly to N_2 fixation in intertidal mats from Laguna Ojo de Liebre and conclude that their activity level was negligible for the N budget of the mat. Instead, the combined data indicate that *Lyngbya* spp. -related cyanobacteria were highly active diazotrophs in the mats at the investigated time.

Conflict of Interest

The authors declare no conflict of interest.

Acknowledgements

We thank Angela Detweiler, Jan Dolinsek, Mike Kubo and Christina Ramon for their excellent technical assistance, José Q García-Maldonado for his assistance in the field, Andrew McDowell at UC Berkeley for IRMS analyses, and Stephanie A Eichorst for helpful comments on the manuscript. We are grateful for access to the field site and for the logistical support provided by Exportadora de Sal, S.A. de C.V. This work was performed under Fishery Permit DAPA/2/080310/734 granted by the National Commission of Aquaculture and Fishery of the Ministry of Agriculture, Livestock, Rural Development, Fisheries and Food (Mexico). Work at LLNL was performed under the auspices of the DOE under contract DE-AC52-07NA27344. Work at LBNL was performed under the auspices of the DOE under contract DE-AC02-05CH11231. This material is based upon work supported by the U.S. Department of Energy, Office of Science, Office of Biological and Environmental Research, Genomic Sciences Program, under contract number SCW1039. This work was further financially supported by the German Research Foundation (Deutsche Forschungsgemeinschaft) (to DW) and the Austrian Science Fund (FWF) (P 25700-B20 to DW). FB and MW were supported by the European Research Council (Advanced Grant Nitrification Reloaded (NITRICARE) 294343).

References

Baumgartner LK, Reid RP, Dupraz C, Decho AW, Buckley DH, Spear JR *et al.* (2006). Sulfate reducing bacteria in microbial mats: changing paradigms, new discoveries. *Sediment Geol* **185**: 131–145.

Bebout BM, Fitzpatrick MW, Paerl HW. (1993). Identification of the sources of energy for nitrogen fixation and physiological characterization of nitrogen-fixing members of a marine microbial mat community. *Appl Environ Microbiol* **59**: 1495–1503.

Bebout BM, Paerl HW, Bauer JE, Canfield DE, Des Marais DJ. (1994). Nitrogen cycling in microbial

mat communities: the quantitative importance of N-fixation and other sources of N for primary productivity. In: Stal LJ, Caumette P (eds) *Microbial Mats*. Springer-Verlag: Berlin, pp 265–272.

Bergman B, Gallon JR, Rai AN, Stal LJ. (1997). N_2 fixation by non-heterocystous cyanobacteria. *FEMS Microbiol Rev* **19**: 139–185.

Burow LC, Woebken D, Marshall IPG, Lindquist EA, Bebout BM, Prufert-Bebout L *et al.* (2013). Anoxic carbon flux in photosynthetic microbial mats as revealed by metatranscriptomics. *ISME J* **7**: 817–829.

Burow LC, Woebken D, Bebout BM, McMurdie PJ, Singer SW, Pett-Ridge J *et al.* (2012). Hydrogen production in photosynthetic microbial mats in the Elkhorn Slough estuary, Monterey Bay. *ISME J* **6**: 863–874.

Canfield DE, Des Marais DJ. (1991). Aerobic sulfate reduction in microbial mats. *Science* **251**: 1471–1473.

Chen YB, Dominic B, Mellon MT, Zehr JP. (1998). Circadian rhythm of nitrogenase gene expression in the diazotrophic filamentous nonheterocystous cyanobacterium *Trichodesmium* sp. strain IMS 101. *J Bacteriol* **180**: 3598–3605.

Cliff JB, Gaspar DJ, Bottomley PJ, Myrold DD. (2002). Exploration of inorganic C and N assimilation by soil microbes with time-of-flight secondary ion mass spectrometry. *Appl Environ Microbiol* **68**: 4067–4073.

de Bont JAM. (1976). Oxidation of ethylene by soil bacteria. *A Van Leeuw J Microb* **42**: 59–71.

Dekas AE, Poretsky RS, Orphan VJ. (2009). Deep-sea archaea fix and share nitrogen in methane-consuming microbial consortia. *Science* **326**: 422–426.

Elsgaard L. (2013). Reductive transformation and inhibitory effect of ethylene under methanogenic conditions in peat-soil. *Soil Biol Biochem* **60**: 19–22.

Everroad RC, Woebken D, Singer SW, Burow LC, Kyrpides N, Woyke T *et al.* (2013). Draft genome sequence of an oscillatorian cyanobacterium, Strain ESFC-1. *Genome Announc* **1**: e00527–13.

Fike DA, Gammon CL, Ziebis W, Orphan VJ. (2008). Micron-scale mapping of sulfur cycling across the oxycline of a cyanobacterial mat: a paired nanoSIMS and CARD-FISH approach. *ISME J* **2**: 749–759.

Fleming ED, Bebout BM, Castenholz RW. (2007). Effects of salinity and light on the resumption of photosynthesis in rehydrated cyanobacterial mats from Baja California Sur, Mexico. *J Phycol* **43**: 15–24.

Foster RA, Kuypers MMM, Vagner T, Paerl RW, Musat N, Zehr JP. (2011). Nitrogen fixation and transfer in open ocean diatom-cyanobacterial symbioses. *ISME J* **5**: 1484–1493.

Gaby JC, Buckley DH. (2011). A global census of nitrogenase diversity. *Environ Microbiol* **13**: 1790–1799.

Griffiths MSH, Gallon JR. (1987). The diurnal pattern of dinitrogen fixation by cyanobacteria *in situ*. *New Phytol* **107**: 649–657.

Halm H, Musat N, Lam P, Langlois R, Musat F, Peduzzi S *et al.* (2009). Co-occurrence of denitrification and nitrogen fixation in a meromictic lake, Lake Cadagno (Switzerland). *Environ Microbiol* **11**: 1945–1958.

Herbert RA. (1999). Nitrogen cycling in coastal marine ecosystems. *FEMS Microbiol Rev* **23**: 563–590.

Javor BJ, Castenholz RW. (1984). Productivity studies of microbial mats, Laguna Guerrero Negro, Mexico. In: Cohen Y, Castenholtz RW, Halvorson HO (eds) *Microbial Mats: Stromatolites*. Alan R. Liss Inc.: New York, NY, USA, pp 149–170.

Kim K, Zhang Y, Roberts GP. (1999). Correlation of activity regulation and substrate recognition of the ADP-ribosyltransferase that regulates nitrogenase activity in *Rhodospirillum rubrum*. *J Bacteriol* **181**: 1698–1702.

Koene-Cottaar FHM, Schraa G. (1998). Anaerobic reduction of ethene to ethane in an enrichment culture. *FEMS Microbiol Ecol* **25**: 251–256.

Lechene C, Hillion F, McMahon G, Benson D, Kleinfeld AM, Kampf JP *et al.* (2006). High-resolution quantitative imaging of mammalian and bacterial cells using stable isotope mass spectrometry. *J Biol* **5**: 20.

Lechene CP, Luyten Y, McMahon G, Distel DL. (2007). Quantitative imaging of nitrogen fixation by individual bacteria within animal cells. *Science* **317**: 1563–1566.

Lee JZ, Burow LC, Woebken D, Everroad RC, Kubo MD, Spormann AM *et al.* (2014). Fermentation couples *Chloroflexi* and sulfate-reducing bacteria to *Cyanobacteria* in hypersaline microbial mats. *Front Microbiol* **5**: 61.

Loy A, Lehner A, Lee N, Adamczyk J, Meier H, Ernst J *et al.* (2002). Oligonucleotide microarray for 16S rRNA gene-based detection of all recognized lineages of sulfate-reducing prokaryotes in the environment. *Appl Environ Microbiol* **68**: 5064–5081.

Lücker S, Steger D, Kjeldsen KU, MacGregor BJ, Wagner M, Loy A. (2007). Improved 16S rRNA-targeted probe set for analysis of sulfate-reducing bacteria by fluorescence *in situ* hybridization. *J Microbiol Meth* **69**: 523–528.

Minz D, Fishbain S, Green SJ, Muyzer G, Cohen Y, Rittmann BE *et al.* (1999). Unexpected population distribution in a microbial mat community: sulfate-reducing bacteria localized to the highly oxic chemocline in contrast to a eukaryotic preference for anoxia. *Appl Environ Microbiol* **65**: 4659–4665.

Moisander PH, Shiue L, Steward GF, Jenkins BD, Bebout BM, Zehr JP. (2006). Application of a *nifH* oligonucleotide microarray for profiling diversity of N_2-fixing microorganisms in marine microbial mats. *Environ Microbiol* **8**: 1721–1735.

Omoregie EO, Crumbliss LL, Bebout BM, Zehr JP. (2004a). Determination of nitrogen-fixing phylotypes in *Lyngbya* sp. and *Microcoleus chthonoplastes* cyanobacterial mats from Guerrero Negro, Baja California, Mexico. *Appl Environ Microbiol* **70**: 2119–2128.

Omoregie EO, Crumbliss LL, Bebout BM, Zehr JP. (2004b). Comparison of diazotroph community structure in *Lyngbya* sp. and *Microcoleus chthonoplastes* dominated microbial mats from Guerrero Negro, Baja, Mexico. *FEMS Microbiol Ecol* **47**: 305–308.

Oremland RS. (1981). Microbial formation of ethane in anoxic estuarine sediments. *Appl Environ Microbiol* **42**: 122–129.

Oremland RS, Capone DG. (1988). Use of ''specific'' inhibitors in biogeochemistry and microbial ecology. *Adv Microb Ecol* **10**: 285–383.

Paerl HW, Prufert LE, Ambrose WW. (1991). Contemporaneous N_2 fixation and oxygenic photosynthesis in the nonheterocystous mat-forming cyanobacterium *Lyngbya aestuarii*. *Appl Environ Microbiol* **57**: 3086–3092.

Paerl HW, Fitzpatrick M, Bebout BM. (1996). Seasonal nitrogen fixation dynamics in a marine microbial mat:

Potential roles of cyanobacteria and microheterotrophs. *Limnol Oceanogr* **41**: 419–427.

Pernthaler A, Pernthaler J, Amann R. (2002). Fluorescence *in situ* hybridization and catalyzed reporter deposition for the identification of marine bacteria. *Appl Environ Microbiol* **68**: 3094–3101.

Pinckney JL, Paerl HW. (1997). Anoxygenic photosynthesis and nitrogen fixation by a microbial mat community in a Bahamian hypersaline lagoon. *Appl Environ Microbiol* **63**: 420–426.

Ploug H, Adam B, Musat N, Kalvelage T, Lavik G, Wolf-Gladrow D *et al.* (2011). Carbon, nitrogen and O_2 fluxes associated with the cyanobacterium *Nodularia spumigena* in the Baltic Sea. *ISME J* **5**: 1549–1558.

Polz MF, Cavanaugh CM. (1998). Bias in template-to-product ratios in multitemplate PCR. *Appl Environ Microbiol* **64**: 3724–3730.

Popa R, Weber PK, Pett-Ridge J, Finzi JA, Fallon SJ, Hutcheon ID *et al.* (2007). Carbon and nitrogen fixation and metabolite exchange in and between individual cells of *Anabaena oscillarioides*. *ISME J* **1**: 354–360.

Rothrock Jr MJ, Garcia-Pichel F. (2005). Microbial diversity of benthic mats along a tidal desiccation gradient. *Environ Microbiol* **7**: 593–601.

Stal LJ, Bergman B. (1990). Immunological characterization of nitrogenase in the filamentous non-heterocystous cyanobacterium *Oscillatoria limosa*. *Planta* **182**: 287–291.

Stal LJ, Krumbein WE. (1981). Aerobic nitrogen fixation in pure cultures of a benthic marine *Oscillatoria* (cyanobacteria). *FEMS Microbiol Lett* **11**: 295–298.

Stal LJ, Grossberger S, Krumbein WE. (1984). Nitrogen fixation associated with the cyanobacterial mat of a marine laminated microbial ecosystem. *Mar Biol* **82**: 217–224.

Steppe TF, Olson JB, Paerl HW, Litaker RW, Belnap J. (1996). Consortial N_2 fixation: a strategy for meeting nitrogen requirements of marine and terrestrial cyanobacterial mats. *FEMS Microbiol Ecol* **21**: 149–156.

Steppe TF, Paerl HW. (2002). Potential N_2 fixation by sulfate-reducing bacteria in a marine intertidal microbial mat. *Aquat Microb Ecol* **28**: 1–12.

Suzuki MT, Giovannoni SJ. (1996). Bias caused by template annealing in the amplification of mixtures of 16S rRNA genes by PCR. *Appl Environ Microbiol* **62**: 625–630.

Wang Q, Garrity GM, Tiedje JM, Cole JR. (2007). Naive Bayesian classifier for rapid assignment of rRNA sequences into the new bacterial taxonomy. *Appl Environ Microbiol* **73**: 5261–5267.

Woebken D, Burow LC, Prufert-Bebout L, Bebout BM, Hoehler TM, Pett-Ridge J *et al.* (2012). Identification of a novel cyanobacterial group as active diazotrophs in a coastal microbial mat using NanoSIMS analysis. *ISME J* **6**: 1427–1439.

Zehr JP, Mellon M, Braun S, Litaker W, Steppe T, Paerl HW. (1995). Diversity of heterotrophic nitrogen fixation genes in a marine cyanobacterial mat. *Appl Environ Microbiol* **61**: 2527–2532.

Zehr JP, Turner PJ. (2001). Nitrogen fixation: nitrogenase genes and gene expression. In: Paul JH (eds) *Methods in Microbiology*. Academic Press: New York, NY, USA, pp 271–286.

Zehr JP, Jenkins BD, Short SM, Steward GF. (2003). Nitrogenase gene diversity and microbial community structure: a cross-system comparison. *Environ Microbiol* **5**: 539–554.

Supplementary Information accompanies this paper on The ISME Journal website (http://www.nature.com/ismej)